Hindawi
Journal of Mathematics
Volume 2023, Article ID 9996556, 18 pages
https://doi.org/10.1155/2023/9996556

Research Article

Option Pricing by Willow Tree Method for Generalized Hyperbolic Lévy Processes

Hongying Wu,[1] Zhiqiang Zhou ,[2] and Caijuan Kang[2]

[1]*School of Mathematics and Information Science, Xiangnan University, Chenzhou 423000, China*
[2]*School of Economics and Management, Xiangnan University, Chenzhou 423000, China*

Correspondence should be addressed to Zhiqiang Zhou; zq.zhou@xnu.edu.cn

Received 10 May 2023; Revised 11 September 2023; Accepted 28 September 2023; Published 17 October 2023

Academic Editor: Barbara Martinucci

In this paper, a new approach is proposed to construct willow tree (WT) for generalized hyperbolic (GH) Lévy processes. There are two advantages of our proposed approach compared to the classical WT methods. Firstly, it avoids the moments matching from Johnson curve in the known WT construction. Secondly, the error of European option pricing is only determined by time partition Δt under some conditions. Since the moments of Lévy measure are removed from this algorithm, our approach improves the stability and accuracy of WT in option pricing. Numerical experiments support our claims. Moreover, the new approach can be extended to other Lévy processes if their characteristic functions are expressed by explicit forms.

1. Introduction

To provide more modeling tools on jump types, the Lévy process is a generalization of the diffusion processes by allowing infinite jump activity. The standard form of the Lévy process assumes stationary increments, hence resulting in nice analytic tractability. The assumption of Lévy processes makes it a good choice for pricing equity derivatives. Generalized hyperbolic (GH, see [1]) process is a class of Lévy processes with wide application in financial field. Variance gamma (VG, see [2, 3]) and normal inverse gamma (NIG, see [4–7]) processes are two special cases of the GH model. VG and NIG models can be obtained from a randomized time-changed clock. The time-changed processes and general Lévy processes exhibit stochastic volatility such that they become capable of capturing volatility smile, smile skew, and term structure of the smile. Also, the hyperbolic (HYP) distribution and the Gauss normal (GN) distribution are viewed as subclasses of the GH model.

Currently, there are five popular numerical methods to price options under Lévy processes, binomial tree methods (BTMs, see [3, 8, 9]), finite difference methods (FDMs, see [10–13]), Monte Carlo methods (MCM, see [14]), FFT-based transformation methods (see [15–18]), and cosine-willow tree methods (see [19]). For BTMs and WTMs, computing transition probabilities (TPs) is an insurmountable barrier. Although a few literature studies discuss BTMs and WTMs for Lévy processes, the accuracy and computational efficiency of them are needed to be enhanced. To use FDMs to valuate options, corresponding partial integral-differential equations (PIDEs) should be established. Generally, PIDEs governed by Lévy processes are very complicated such that PIDEs are limited in several options. The Monte Carlo method is straightforward, but it is quite time-consuming to generate random samples for the Lévy process. The FFT-based transformation method is the most popular one in option pricing, such as the COS method (see [16]) and PROJ method (see [17]). The COS method employs a cosine series expansion on the risk-neutral return density and estimates the European option price based on the numerical integration on $(-\infty, +\infty)$. However, it is hard to determine a proper finite interval $[a, b]$ to truncate $(-\infty, +\infty)$ for the integration (see [15, 18, 20]) and is hard to be extended to path-dependent options. The PROJ method overcomes these shortcomings and is extendable to Asian options, variance swaps, and American options but its extendability is still limited compared to the Cosine-willow tree method.

The key of the WT method for option pricing is to construct willow tree structure (see [13]). In this paper, we propose WT algorithms for GH Lévy processes. The main contributions of this paper are fourfolds.

(1) An numerical algorithm is proposed to compute the probability density functions (PDFs) and cumulative distribution probabilities (CDPs) from the characteristic functions (CDs) of GH processes. This algorithm is unified and suitable for all GH subclass models.

(2) In FFT-based transformation methods (see [15, 18, 20, 21]), it is hard to find a proper finite interval $[a, b]$ to truncate the integration over $(-\infty, +\infty)$. While in the WT method, we propose an adaptive integration method in which the appropriate integral interval $[a, b]$ is automatically found. In determining $[a, b]$, the WT algorithm does not consume too much extra computational effort.

(3) By setting appropriate m discrete stock prices at each time t_n and calculating transform probabilities $p_{ij}^{(n)}$ from t_n to t_{n+1}, WT structure is constructed. Unlike Ma et al. [19], it is not needed to estimate the k-order moments of the GH Lévy model when selecting m nodes at each time t_n. The determination of m nodes at each time t_n only relies on PDFs or CDFs of GH processes, which makes our WT programming run fast than those developed by Ma et al. (see [19]).

(4) The convergence rate $O(\Delta t)$ of European option on the WT structure is proved. Numerical experiments show that American options computed by our WT algorithm are also convergent for time partition Δt and the underlying partition number m.

The remaining parts of this paper are arranged as follows. Basic conceptions are reviewed in Section 2. Calculation of PDFs and CDFs is illustrated in Section 3. The convergence analysis for European options is discussed in Section 4. Numerical examples of GH Lévy processes are carried out in Section 5. Some conclusions and remarks are given in the final section.

2. GH Lévy Processes

In option pricing with non-Gaussian processes, the asset price process S_t is defined as an exponential Lévy process X_t, i.e.,

$$S_t = S_0 e^{(r+\omega_{\mathrm{GH}})t+X_t}, \tag{1}$$

where r is the risk-free interest rate and ω_{GH} is a martingal adjustment parameter under risk-neutral measure $\mathbb{Q}$. Under the GH Lévy processes (1), option pricing becomes more complicated than the classical BS model. For FDMs, partial integral-differential equations (PIDEs) are needed, and then numerical schemes should be designed to solve these PIDEs. For BTMs and WTMs, calculating transform probabilities (TPs) cannot be avoided. Formulating PIDEs, designing numerical schemes for PIDEs, and calculating TPs for BTMs and WTMs are not easy tasks.

We consider the generalized hyperbolic (GH) model (see [1, 22, 23]) whose characteristic function with five parameters $(\alpha, \beta, \delta, \mu, \lambda)$ is defined by the following equation:

$$\phi^{GH}(u) = e^{i\mu u}\left(\frac{\alpha^2 - \beta^2}{\alpha^2 - (\beta + iu)^2}\right)^{\lambda/2} \frac{K_\lambda\left(\delta\sqrt{\alpha^2 - (\beta + iu)^2}\right)}{K_\lambda\left(\delta\sqrt{\alpha^2 - \beta^2}\right)}, \tag{2}$$

where $K_\lambda(\cdot)$ is the λ^{th}order-modified Bessel function of the second kind. The density function of the GH model $\rho^{\mathrm{GH}}(x)$ can be derived as follows:

$$\rho^{\mathrm{GH}}(x) = \frac{\left(\alpha^2 - \beta^2\right)^{\lambda/2}\left[\delta^2 + (x-\mu)^2\right]^{\lambda/2-1/4}}{\sqrt{2\pi}(\alpha\delta)^{\lambda-1/2}\delta^{1/2}K_\lambda\left(\delta\sqrt{\alpha^2 - \beta^2}\right)} e^{\beta(x-\mu)} K_{\lambda-1/2}\left(\alpha\sqrt{\delta^2 + (x-\mu)^2}\right). \tag{3}$$

In CFs (2), $\mu \in \mathbb{R}$ and the other parameters satisfy the following constraints:

$$\begin{cases} \delta \geq 0, \alpha > 0, |\beta| < \alpha \text{ if } \lambda > 0, \\ \delta > 0, \alpha > 0, |\beta| < \alpha \text{ if } \lambda = 0, \\ \delta > 0, \alpha \geq 0, |\beta| \leq \alpha \text{ if } \lambda < 0. \end{cases} \tag{4}$$

The GH distribution embeds various distributions under special choices of the parameters. The parameter λ determines the subclass of the GH distribution. When $\lambda = 1$, the GH distribution reduces to the hyperbolic distribution (HYP) whose logarithm of density is a hyperbolic. In addition, when $\delta \longrightarrow \infty$ and $\delta/\alpha \longrightarrow \sigma^2$, the GH distribution reduces to the Gauss normal (GN) distribution. Furthermore, when $\delta = 0$ and $\mu = 0$, the GH distribution becomes the variance gamma (VG) distribution; when $\lambda = -1/2$, it becomes the normal inverse Gaussian (NIG) distribution. Table 1 gives the four different categories of the GH model.

Figure 1 plots the graphs of $\rho^{\mathrm{GH}}(x)$ with different values of parameters. From the Figure, we see the shape of tail, skewness, and kurtosis of the GH distribution which are controlled by α, β, and δ, respectively.

Because the GH law is infinitely divisible, one can construct a GH Lévy process X_t whose distribution at fixed time t has characteristic function ϕ_{X_t}. The characteristic function is described by the following equation (see [22]):

Table 1: Special cases of GH distribution.

Parameters	Type of distribution
$\lambda = 1$	HYP: hyperbolic distribution
$\lambda = -1/2$	NIG: normal inverse Gaussian distribution
$\delta/\alpha \longrightarrow \sigma^2$ and $\delta \longrightarrow \infty$	GN: Gaussian normal distribution
$\delta \longrightarrow 0$, $\mu \longrightarrow 0$	VG: variance gamma distribution

$$\begin{aligned}\phi_{X_t}(u) &= \mathbb{E}\left[e^{iuX_t}\right] \\ &= \int_{-\infty}^{\infty} e^{iux}\rho^{\mathrm{GH}_t}(x)dx \\ &= \left[\phi^{GH}(u)\right]^t: \\ &= e^{i\mu ut}\left[\widetilde{\phi}^{GH}(u)\right]^t.\end{aligned} \tag{5}$$

where $i = \sqrt{-1}$, $\rho^{\mathrm{GH}_t}(x)$ is the density function of GH process at time t, and $\phi^{GH}(u)$ is defined as (2). The function $\widetilde{\phi}^{GH}(u) = \phi^{GH}(u)e^{-i\mu u}$ is the part in which the oscillating factor $e^{i\mu u}$ is removed. The characteristic exponent of GH process is as follows:

$$\begin{aligned}\psi_X(u) &= \frac{1}{t}\log\phi_{X_t}(u) \\ &= \log\phi^{GH}(u).\end{aligned} \tag{6}$$

Since a Lévy process is an infinitely divisible distribution, the Lévy-Khintchine theorem (see Theorem 8.1 in [24]) for an infinitely divisible distribution can be applied to establish the characteristic exponent $\psi_X(u)$ of a Lévy process X_t. $\psi_X(u)$ admits the Lévy–Khintchine representation, i.e.,

$$\psi_X(u) = i\mu u - \frac{\sigma^2 u^2}{2} - \int_{\mathbb{R}/\{0\}}\left(1 - e^{iux} + iux1_{|x|<1}\right)\Pi(\mathrm{d}x). \tag{7}$$

The Lévy measure $\Pi(\mathrm{dx})$ is defined on the real domain excluding zero with $\Pi(\{0\}) = 0$. The triplet (μ, σ^2, Π) is called the Lévy characteristic of X_t, where $\mu \in \mathbb{R}$ is the constant drift, $\sigma > 0$ is the constant volatility of the continuous component, and Π is the Lévy measure that represents the expected number of jumps per unit time. In GH model (1), the parameter σ is set as zero. The Lévy measure of the GH model has no explicit analytic form and it can be expressed only in terms of integrals (see [25]). To satisfy the martingale condition $\mathbb{E}_{\mathbb{Q}}[S_t|S_0] = S_0$ in SDE (1), the adjustment parameter is chosen as $\omega_{\mathrm{GH}} = -\psi_X(-i)$.

The density function $\rho^{\mathrm{GH}_t}(x)$ can be restored from characteristic function $\phi_{X_t}(u)$ by numerical inverse integral. Once the characteristic function (5) is given, the density function $\rho^{\mathrm{GH}_t}(x)$ is expressed as

$$\begin{aligned}\rho^{\mathrm{GH}_t}(x) &= \frac{1}{2\pi}\int_{-\infty}^{\infty} e^{-iux}\phi_{X_t}(u)du \\ &= \frac{1}{2\pi}\int_{-\infty}^{\infty} e^{-iu(x-\mu t)}\left[\widetilde{\phi}_X(u)\right]^t du,\end{aligned} \tag{8}$$

with definition $\widetilde{\phi}_X(u)$ in (5). We note that the integral factor $e^{-iu(x-\mu t)}$ is the part with high frequency oscillation, whereas $\widetilde{\phi}_X(u)$ is decaying quickly as $|u| \longrightarrow \infty$. This observation is very important for computing the density function $\rho^{\mathrm{GH}_t}(x)$, numerically.

3. Willow Tree Algorithm

3.1. Willow Tree Structure. A willow tree for the GH model is represented by $\left\{X_i^n, S_i^n, p_{ij}^{(n)}\right\}$, where X_i^n is discrete nodes of Lévy processes X_t at time t_n, $S_i^n = S_0 e^{(r+\omega_{\mathrm{GH}})t + X_i^n}$ is underlying prices, and $p_{ij}^{(n)}$ is the transition probability. As shown in Figure 2, there are two main stages to construct a willow tree: (i) selecting the discrete tree nodes, X_i^n ($i = 1, 2, 3, \cdots, m$ and $n = 1, 2, \cdots, N$), for X_t at each time t_n and (ii) determining the transition probability, $p_{ij}^{(n)}$, from X_i^n at t_n to X_j^{n+1} at t_{n+1} on a discrete time points $0 = t_0 < t_1 < t_2 < \cdots < t_N = T$ with $t_n = n\Delta t$ and $\Delta t = T/N$, $n = 1, 2, \cdots, N$.

Firstly, the discrete pairs $\{(X_i^n, q_i)\}$ $(i = 1, 2, \cdots, m; n = 1, 2, \ldots, N)$ are selected to approximate the distribution of X_t at time t_n. The cumulative distribution functions (CDFs) of $X_t = X_i^n$ at t_n are computed by

$$F^n(X_i^n) = \int_{-\infty}^{X_i^n} \rho^{\mathrm{GH}_{t_n}}(x)dx \coloneqq q_i, \quad i = 1, 2, \ldots, m; n = 1, 2, \ldots, N. \tag{9}$$

After setting discrete probabilities,

$$q_i = \frac{(i - 0.5)}{m}, \quad i = 1, 2, \cdots, m, \tag{10}$$

we can numerically determine X_i^n by solving equation (9) if the integral can be computed efficiently and accurately. Very different from the classical WT method (see [19]), the determination of nodes X_i^n avoids computing k-order moments of X_t. This modification makes our algorithms more easily and widely available for Lévy processes.

Secondly, the transition probability between two consecutive discrete times t_n and t_{n+1} is computed as

$$\begin{aligned}p_{ij}^{(n)} &= \mathbb{P}\left(\Delta_{n,ij}^{(\mathrm{down})} \le X^{n+1} - X_i^n \le \Delta_{n,ij}^{(up)}\right) \\ &= \int_{\Delta_{n,ij}^{(down)}}^{\Delta_{n,ij}^{(up)}} \rho^{\mathrm{GH}_{\Delta t}}(x)dx,\end{aligned} \tag{11}$$

with increments of Lévy processes. Increments $\Delta_{n,ij}^{(\mathrm{down})}$ and $\Delta_{n,ij}^{(\mathrm{up})}$ are defined as

$$\begin{aligned}\Delta_{n,ij}^{(\mathrm{down})} &= \frac{1}{2}\left(X_{j-1}^{n+1} + X_j^{n+1}\right) - X_i^n, \\ \Delta_{n,ij}^{(up)} &= \frac{1}{2}\left(X_j^{n+1} + X_{j+1}^{n+1}\right) - X_i^n.\end{aligned} \tag{12}$$

In computation (11), $n = 0, 1, \ldots, N-1$ and $i, j = 1, 2, \ldots, m$, and an exception is that $X_i^0 \equiv 0$ with $i \equiv 1$.

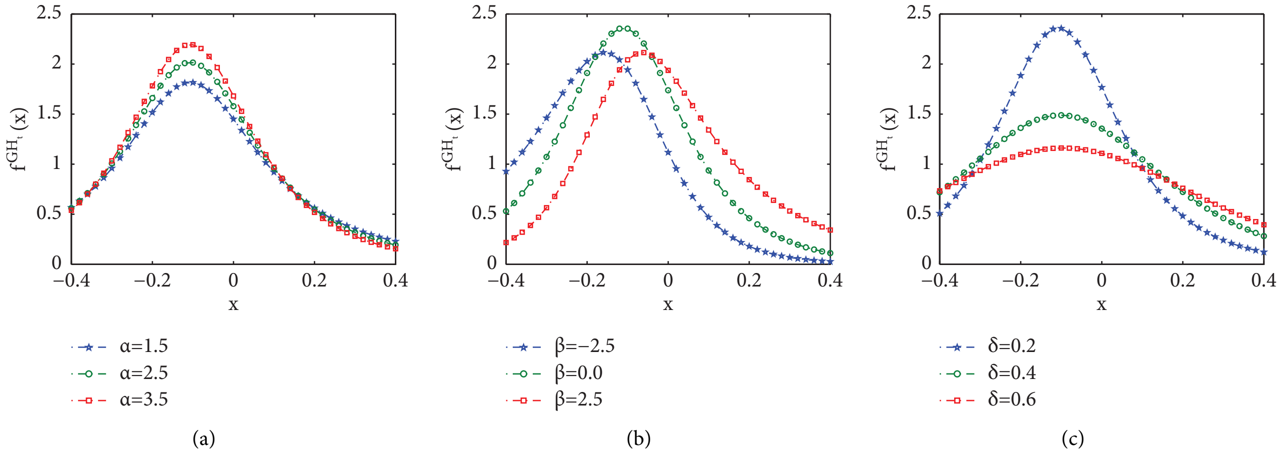

FIGURE 1: Density function $\rho^{\mathrm{GH}}(x)$ with parameters $\lambda = -1/2, \alpha = 4.5, \beta = 0.15, \mu = -0.1$, and $\delta = 0.2$: (a) density functions with different α, (b) density functions with different β, and (c) density functions with different δ.

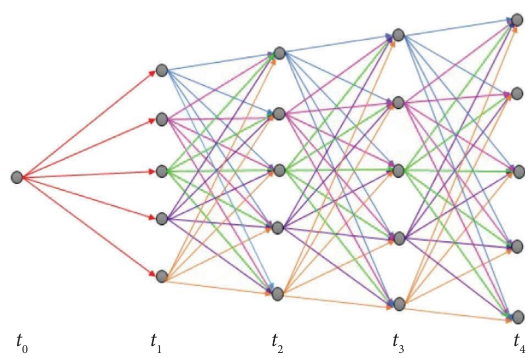

FIGURE 2: Graphical depiction of the willow tree lattice with 5 possible asset prices and 4 discrete times.

There are two most important aspects in willow tree construction. One is to calculate PDF $\rho^{\mathrm{GH}_{t_n}}(x)$ and then generate willow tree nodes $\{X_i^n\}$ and another is to compute transition probability $p_{ij}^{(n)}$ via $\rho^{\mathrm{GH}_{\Delta t}}(x)$ for given Δt. Once the PDFs $\rho^{\mathrm{GH}_{t_n}}(x)$ and $\rho^{\mathrm{GH}_{\Delta t}}(x)$ are computed, the willow tree algorithm can be applied in some types of option pricing, such as European, American, Asian options, and so on.

3.2. Numerical Computing of PDFs and CDFs for GH Processes. Firstly, we numerically compute the PDFs $\rho^{\mathrm{GH}_t}(x)$ defined by (8). There is a challenge for the high frequency oscillation of integral kernel $e^{-iu(x-\mu t)}$ when the value of $(x-\mu t)$ is large. We consider the following truncation:

$$\rho^{\mathrm{GH}_t}(x) = \frac{1}{2\pi}\int_{-\infty}^{\infty} e^{-iu(x-\mu t)}\left[\widetilde{\phi}_X(u)\right]^t du \approx \frac{1}{2\pi}\int_{A}^{B} e^{-iu(x-\mu t)}\left[\widetilde{\phi}_X(\mathrm{u})\right]^{\mathrm{t}} du. \tag{13}$$

In the above expression, A is a sufficiently large negative number and B is a large enough positive constant. Let partition nodes $u_k = A + k\Delta u$ for $k = 0, 1, \cdots, M$ with $\Delta u = (B - A)/M$. Then, $\rho^{\mathrm{GH}_t}(x)$ can be numerically integrated (NI), i.e.,

$$\begin{aligned} \mathrm{NI:} &\approx \frac{1}{2\pi}\sum_{k=0}^{M-1}\theta_k^t \int_{u_k}^{u_{k+1}} e^{-iu(x-\mu t)}du = \frac{1}{2\pi i(\mu t - x)}\sum_{k=0}^{M-1}\theta_k^t C_k^t \\ &\coloneqq \widetilde{\rho}^{\mathrm{GH}_t}(x), \end{aligned} \tag{14}$$

with notation

$$\begin{cases} \theta_k^t = \frac{1}{2}\left(\left[\widetilde{\phi}_X(u_k)\right]^t + \left[\widetilde{\phi}_X(u_{k+1})\right]^t\right), \\ C_k^t = i(\mu t - x)\int_{u_k}^{u_{k+1}} e^{-i(x-\mu t)u} du = e^{-i(x-\mu t)u}\Big|_{u=u_k}^{u=u_{k+1}}. \end{cases} \tag{15}$$

Remark 1. The numerical formula (14) plays a key role for both $t = t_n$ and $t = \Delta t$. (i) Let $t = t_n$, we can calculate CDFs $F^n(X_i^n)$ at each time t_n. (ii) Nodes $\{X_i^n\}$ can be determined by solving $F^{t_n}(X_i^n) = q_i$ for $i = 1, 2, \cdots, m$ (see expression (9)). (iii) Transition probabilities $p_{ij}^{(n)}$ (see formula (11) can be calculated by numerical approximation with $t = \Delta t$. (iv) Using formula (14), we can expand the range of [A, B] until the result $\rho^{\mathrm{GH}_t}(x)$ does not change much, which can be seen as an adaptive algorithm.

Remark 2. Since the absolute values of characteristic function $\phi_X(u)$ are decreasing to zero as u tends to $\pm\infty$, the nodes $\{u_k\}$ can be selected as nonuniform, for example,

$$u_k = B\left(\frac{k}{M}\right)^\kappa \text{and } u_k = A\left(\frac{k}{M}\right)^\kappa, \tag{16}$$

with $\kappa > 1$ for $k = 1, 2, \cdots, M$. Using nonuniform nodes $\{u_k\}$, we can achieve more accurate $\widetilde{\rho}^{\mathrm{GH}_t}(x)$ with less nodes.

Next, we compute transition probabilities $p_{ij}^{(n)}$ with definition (11). Taking discrete values $-\infty < x_0 < x_1 < \cdots < x_i = X_i^n$ with sufficiently large negative number x_0 and sufficiently small $\Delta x := = \max_{1\le j\le i}[x_j - x_{j-1}]$, CDFs $F^n(X_i^n)$ are approximated by

$$F^n(X_i^n) \approx \frac{1}{2}\sum_{j=1}^{i}\left[\rho^{GH_{t_n}}(x_{j-1}) + \rho^{GH_{t_n}}(x_j)\right](x_j - x_{j-1}), \tag{17}$$

for $i = 1, 2, \cdots, m$ and $n = 1, 2, \cdots, N$. The transition probability $p_{ij}^{(n)}$ is approximated by

$$p_{ij}^{(n)} = F^{n=1}\left(\Delta_{n,ij}^{(\mathrm{up})}\right) - F^{n=1}\left(\Delta_{n,ij}^{(\mathrm{down})}\right), \tag{18}$$

with $\Delta_{n,ij}^{(\mathrm{up})}$ and $\Delta_{n,ij}^{(\mathrm{down})}$ being denoted by expression (12). Using (9) and (14)–(18), Algorithm 1 describes the details of constructing willow tree $\left\{X_i^n, S_i^n, p_{ij}^{(n)}\right\}$ for GH Lévy processes.

3.3. European and American Options

3.3. European and American Options. After the willow tree $\left\{X_i^n, S_i^n, p_{ij}^{(n)}\right\}$ is constructed, European and American options can be valued on WT backward. Other options (Asian, Lookback, and so on) also can be computed from WT and we omit the details.

Define by V_i^n the option values at time t_n with underlying $S_i^n = S_0 e^{(r+\omega_{\mathrm{GH}})t_n + X_i^n}$. Option values V at $t = 0$ with parameters (S_0, K, T, r) can be computed from willow tree as follows:

$$\begin{cases} V_i^N = f\left(S_i^N\right), \quad \text{for } i = 1, 2, \ldots, m, \\ V_i^n = e^{-r\Delta t}\sum_{j=1}^{m} p_{ij}^{(n)} V_j^{n+1}, \quad \text{for } n = N-1, N-2, \ldots, 1, \\ V(S_0, K, T, r) = e^{-r\Delta t}\sum_{j=1}^{m} p_{1j}^{(0)} V_j^1, \end{cases} \tag{19}$$

where payoff function $f(\xi) = (\xi - K)^+$ for call options, whereas $f(x) = (K - \xi)^+$ for put options.

American option value V at time zero with parameters (S_0, K, T, r) can be determined backward on willow tree.

$$\begin{cases} V_i^N = f\left(S_i^N\right), \quad \text{for } i = 1, 2, \ldots, m; \\ V_i^n = \max\left\{e^{-r\Delta t}\sum_{j=1}^{m} p_{ij}^{(n)} V_j^{n+1}, f\left(S_i^n\right)\right\}, \quad \text{for } n = N-1, N-2, \ldots, 1; \\ V(S_0, K, T, r) = \max\left\{e^{-r\Delta t}\sum_{j=1}^{m} p_{1j}^{(0)} V_j^1, f(S_0)\right\}. \end{cases} \tag{20}$$

American options via willow tree are described in Algorithm 2.

3.4. A Simple Method to Determine m Nodes at Each Time t_n. To generate m nodes X_i^n at each time t_n, it is much time-consuming according to Step 6 in Algorithm 1. We give a simple algorithm to generate m nodes only depending on CDFs $F^n(\cdot)$ (see (17)). Assume $\{X_i^n\}$ as given, the nodes X_i^{n+1} are generated as follows. Find X_i^{n+1} such that

$$\sum_{j=1}^{m} F^{n=1}\left(\Delta_n^{i,j} X\right) = (i - 0.5) := mq_i, \text{with } \Delta_n^{i,j} X = X_i^{n+1} - X_j^n, \tag{21}$$

%% Input parameters
Step 1. Set GH-model parameters $(\alpha, \beta, \mu, \delta, \lambda, T)$.
%% Compute probability density function
Step 2. Set willow tree parameters (N, m) and computational parameters M. N represents the number of time discretization and m represents the number of X-nodes at each time t_n. M is the number in NI formula (14) for PDFs $\rho^{\mathrm{GH}_t}(x)$.
%% Compute probability density function for $t = t_n$ and $t = \Delta t$.
Step 3. Set discrete space nodes $u_k = A + k\Delta u$ with $\Delta u = (B - A)/M$ for $k = 1, 2, \cdots, M$.
Step 4. Compute θ_k^t and C_k^t for $k = 0, 1, \cdots, M - 1$ using formulas (15);
Step 5. According to (14), compute PDFs $\rho^{\mathrm{GH}_t}(x)$ on given points $\{x_i\}_{i=1:\,m}$.
%% Generate WT nodes and compute transition probabilities.
Step 6. According to (17), compute $F^n(X_i^n)$ at each time $t = t_n$. By solving (3.1), determine nodes X_i^n for $n = 1, 2, \cdots, N$ and $i = 1, 2, \cdots, m$.
Step 7. Compute discrete underlying $S_i^n = S_0 e^{(r+\omega_{\mathrm{GH}})t_n + X_i^n}$ for $n = 1, \cdots, N$ and $i = 1, 2, \cdots, m$.
Step 8. Based on (18), compute transition probability $p_{ij}^{(n)}$ for $n = 0, 1, \cdots, N - 1$ and $i, j = 1, 2, \cdots, m$.
Step 9. Willow tree $\left\{X_i^n, S_i^n, p_{ij}^{(n)}\right\}$ for the GH model is constructed.

Algorithm 1: Willow tree construction.

%% Input parameters and prepare willow tree
Step 1. Set willow tree parameters (N, m) and computational parameters M. N represents the number of time discretization and m represents the number of X-nodes at each time t_n. M is the number in NI formula (14) for PDF $\rho^{\mathrm{GH}_t}(x)$.
Step 2. Generate willow tree $\left\{\mathrm{X}_\mathrm{i}^\mathrm{n}, \mathrm{S}_\mathrm{i}^\mathrm{n}, \mathrm{p}_\mathrm{ij}^{(\mathrm{n})}\right\}$ by Algorithm 1.
%% Compute options backward from time t_N to t_1
Step 3. Compute payoff function at time T, i.e., $V_i^N = f(S_i^N)$ for $i = 1, 2, \cdots, m$, where $f(\xi) = (\xi - K)^+$ for call options, whereas $f(x) = (K - \xi)^+$ for put options.
Step 4. For $n = N - 1$ to 1
—— Compute European values $V_i^n(E) = e^{-r\Delta t}\sum_{j=1}^m p_{ij}^{(n)} V_j^{n+1}$ for $i = 1, 2, \cdots, m$
—— Compute exercise values $V_i^n(A) = f(S_i^n)$ for $i = 1, 2, \cdots, m$
—— Take American values $V_i^n = \max\{V_i^n(E), V_i^n(A)\}$ for $i = 1, 2, \cdots, m$
EndFor
%% Output American option $V(S_0, K, T, r)$
Step 5. Calculate option value $V(S_0, K, T, r) = \max\left\{e^{-r\Delta t}\sum_{j=1}^m p_{1j}^{(0)} V_j^1, f(S_0)\right\}$.

Algorithm 2: American option pricing on willow tree.

for $i = 1, 2, \cdots, m$, where $F^{n=1}(\cdot)$ is the CDFs of the GH model (defined in (17)) and $q_i = (i - 0.5)/m$. If the discrete probability distribution $\{F, x\}$ is given with probabilities $F = [F_1, F_2, \cdots, F_L]'$ and corresponding increments $x = [x_1, x_2, \cdots, x_L]'$, then X_i^{n+1} can be obtained by interpolation:

$$X_i^{n+1} = \mathrm{interp}(F, x, mq_i) + X_i^n, \quad i = 1, 2, \cdots, m. \tag{22}$$

Now, we describe the method of generating nodes $\{X_i^n, S_i^n\}$ as in Algorithm 3. Compared with the method proposed by this algorithm avoids to compute the k-moments of X_t. The modification of our algorithm saves much CPU time in willow tree construction.

4. Convergence Analysis

Errors of option pricing from willow tree have two aspects: the errors $\varepsilon(\rho) = \rho^{\mathrm{GH}_t}(x) - \tilde{\rho}^{\mathrm{GH}_t}(x)$ (see (14)) coming from the calculation for PDFs (or CDFs) and the errors from backward computation on willow tree (see (19) and (20)). We give some detailed analysis in this section.

4.1. Errors of PDFs and CDFs. We know that the absolute value of characteristic function $\phi_X(u)$ is decreasing to zero as u tends to $\pm\infty$. So, the error $\varepsilon(\rho)$ can be estimated as follows.

Theorem 3. *Assume that the characteristic function satisfies $|\phi_X(u)| \le \epsilon/2$ for $u \notin (A, B)$, then*

$$\varepsilon(\rho) = \left|\rho^{\mathrm{GH}_t}(x) - \tilde{\rho}^{\mathrm{GH}_t}(x)\right| \le \frac{1}{2\pi|\mu t - x|}\left[\epsilon + \mathcal{O}\left(\frac{1}{M^2}\right)\right], x \ne \mu t, \tag{23}$$

where PDFs $\rho^{\mathrm{GH}_t}(x)$ and estimated PDFs $\tilde{\rho}^{\mathrm{GH}_t}(x)$ are defined by (14) and M is the number of nodes $\{u_k\}$.

Proof. It is obvious that

Step 1. Give the first node $X_1^0 = 0$ and $S_1^0 = S_0$ at time zero.
%% generate CDFs F on nodes x
Step 2. Based on (17), generate discrete distribution $F_j = F^{n=1}(x_j)$ for $j = 0, 2, \cdots, L$. Here, x_0 is a sufficient small number, x_L is a sufficient larger number and $\max_{j=1:\,L}|x_j - x_{j-1}|$ sufficient small.
%% generate X_i^{n+1} for $n = 0, 1, \cdot, N-1$.
Step 3. For $n = 0$: $N-1$, generate X_i^{n+1} by interpolation,
$X_i^{n+1} = \text{interp}(F, x, mq_i) + X_i^n$, $i = 1, 2, \cdots, m$.
END
Step 4. Compute discrete underlying $S_i^n = S_0 e^{(r+\omega_{\text{GH}})t_n + X_i^n}$ and then the nodes $\{X_i^n, S_i^n\}$ of willow tree are generated.

Algorithm 3: Generate nodes $\{X_i^n, S_i^n\}$.

$$\varepsilon(\rho) = \rho^{GH_t}(x) - \widetilde{\rho}^{\text{GH}_t}(x) = \frac{1}{2\pi} \times \left[\int_{-\infty}^{A} e^{-iu(x-\mu t)} g(u;t)du + \int_{B}^{+\infty} e^{-iu(x-\mu t)} g(u;t)du + \int_{A}^{B} [g(u;t) - \overline{g}(u;t)]du\right], \tag{24}$$

where $g(u;t) = [\phi_X(u)]^t$ and $\overline{g}(u;t) = 1/2\,[\phi_X^t(u_k) + \phi_X^t(u_{k+1})]$ for $u \in (u_k, u_{k+1})$. From error estimation of composite trapezoidal rule (see Richard and Dougals Faires [26]), we have

$$\begin{aligned}
|\varepsilon(\rho)| &= \left|\rho^{GH_t}(x) - \widetilde{\rho}^{\text{GH}_t}(x)\right| \le \frac{1}{2\pi} \times \left[\frac{\epsilon}{2}\int_{-\infty}^{A} e^{-iu(x-\mu t)}du + \frac{\epsilon}{2}\int_{B}^{+\infty} e^{-iu(x-\mu t)}du + \int_{A}^{B}[g(u;t) - \overline{g}(u;t)]du\right] \\
&\le \frac{1}{2\pi|\mu t - x|}\left[\frac{\epsilon}{2} + \frac{\epsilon}{2} + \frac{B-A}{12M^2}g_u''(\zeta)\right], \quad \zeta \in (A, B), \\
&= \frac{1}{2\pi|\mu t - x|}\left(\epsilon + \mathcal{O}\left(\frac{1}{M^2}\right)\right), \quad \forall x \ne \mu t,
\end{aligned} \tag{25}$$

which is the result of (23). □

Remark 4. Given $x \in \mathbb{R}$, to ensure the error $\varepsilon(\rho)$ be small enough, $|A|$, B, and M should be taken as large as enough. For given $\varepsilon(\rho)$, a simple choice is to select $|A|$ and B such that

$$\min_{A,B}\left\{|\phi_X(A)|, |\phi_X(B)|\right\} \le \pi\varepsilon(\rho)|\mu\text{t} - \text{x}|, \tag{26}$$

and then find M such that

$$\frac{B-A}{12M^2}\max_{\xi\in[A,B]}\left|g_u''(\xi,t)\right| \le \pi\varepsilon(\rho)|\mu\text{t} - \text{x}|. \tag{27}$$

As an example, Table 2 gives the choices of A, B, M for different values of x and fixed $\varepsilon(\rho) = 10^{-6}$.

4.2. Convergence of Willow Tree for European Option. Denoted by $E_{\Delta t}^{(k)}$ the conditional k^{th} moments of increment $\Delta X = X^{n+1} - X^n$ with given $X^n = X_i^n$, i.e.,

$$E_{\Delta t}^{(k)} = \mathbb{E}\left[\left(X^{n+1} - X_i^n\right)^k\right] = \int_{-\infty}^{+\infty} u^k \rho^{\text{GH}_{\Delta t}}(u)du, k = 1, 2, \ldots, \tag{28}$$

where $\rho^{\text{GH}_{\Delta t}}(u)$ is the PDFs of the increment of X_t at t_{n+1} given $X^n = X_i^n$. For convenience, we give an assumption as follows.

Assumption 5. There exists a positive number H such that

$$h \coloneqq \max_{n,i,j}\left|\Delta_{n,i,j}^{(\text{up})} - \Delta_{n,i,j}^{(\text{down})}\right| \le \frac{H}{m}, \tag{29}$$

for $n = 1, 2, \ldots, N$ and $i, j = 1, 2, \ldots, m$. Here, $\Delta_{n,ij}^{(\text{up})}$ and $\Delta_{n,ij}^{(\text{down})}$ are denoted by expression (12).

Lemma 6. *Assume X_t as a GH Lévy process, then $E[X_t]$ and $Var[X_t]$ have the following results:*

Table 2: Choices of A, B, M for different values of x, fixed $\Delta t = 0.2$ and fixed $\varepsilon(\rho) = 10^{-6}$.

x	A	B	M	x	A	B	M
−1.00	−234	234	26056	1.00	−239	239	30318
−0.10	−260	260	59858	0.10	−291	291	55116
−0.01	−271	271	83034	0.01	−271	271	83034

Parameters of the GH model are set as $\lambda = -2, \alpha = 15, \beta = 8, \delta = 0.3$, and $\mu = 0.7$.

$$\mathbb{E}[X_t] = \mu + \frac{\beta\delta}{\sqrt{\alpha^2-\beta^2}}\frac{K_{\lambda+1}(\zeta)}{K_\lambda(\zeta)},$$

$$\mathrm{Var}[X_t] = \delta^2\left\{\frac{K_{\lambda+1}(\zeta)}{\zeta K_\lambda(\zeta)} + \frac{\beta^2}{\alpha^2-\beta^2}\left[\frac{K_{\lambda+2}(\zeta)}{K_\lambda(\zeta)} - \frac{K_{\lambda+1}(\zeta)}{K_\lambda(\zeta)}\right]^2\right\}, \tag{30}$$

with $\zeta = \delta\sqrt{\alpha^2-\beta^2}$.

Proof. The proof can be seen in Cont and Tankov [27]. □

Lemma 7. *Given X_t following GH Lévy processes, the k^{th} conditional moment of increment $\Delta X = X^{n+1} - X_i^n$ has estimation $E_{\Delta t}^{(k)} = O((\Delta t)^k)$ for $k \geq 1$.*

Proof. Given the characteristic exponent $\psi_X(u)$ of X_t and characteristic function $\phi_{X_{\Delta t}}(u)$, it implies that

$$\frac{d^{k+1}\phi_{X_{\Delta t}}(u)}{du^{k+1}} = \Delta t\sum_{\ell=0}^{k}\frac{k!}{\ell!(k-\ell)!}\left[\frac{d^\ell\phi_{X_{\Delta t}}(u)}{du^\ell}\right]\left[\frac{d^{k+1-\ell}\psi_X(u)}{du^{k+1-\ell}}\right], \quad k = 0, 1, \ldots. \tag{31}$$

Since $E_{\Delta t}^{(\ell)} = (-i)^\ell[d^\ell\phi_{\Delta X}(u)/du^\ell]|_{u=0}$, we have

$$E_{\Delta t}^{(k+1)} = \Delta t\sum_{\ell=0}^{k}\frac{k!}{\ell!(k-\ell)!}c_{k+1-\ell}E_{\Delta t}^{(\ell)}, \tag{32}$$

where $c_{k+1-\ell} = (-i)^{k+1-\ell}[d^{k+1-\ell}\psi_X(u)/du^{k+1-\ell}]|_{u=0}$ is the cumulants of X_t. Thus, we obtain $E_{\Delta t}^{(k)} = O((\Delta t)^k)$ for $k \geq 1$.

The following lemma gives an estimation of $R_{\Delta t,m}^{(k)}$, the error between k^{th} moments, and their discrete approximations. □

Lemma 8. *Given X_t following GH Lévy processes, under Assumption 5, i.e., h is bounded by H/m with constant H, the errors between $E_{\Delta t}^{(k)}$ and its discrete approximations $\sum_{j=1}^m p_{ij}^{(n)}(\Delta X_{ij}^n)^k$ with $\Delta = X_j^{n+1} - X_i^n$ can be estimated by*

$$\left|R_{\Delta t,m}^{(k)}\right| \equiv \left|\sum_{j=1}^m p_{ij}^{(n)}\left(\Delta X_{ij}^n\right)^k - E_{\Delta t}^{(k)}\right| = O\left(\frac{\sqrt{\Delta t}}{m}\right), k \geq 1. \tag{33}$$

Proof. Using the following integral operator:

$$\mathcal{I}(f) := \int_{\Delta_{n,ij}^{(\mathrm{down})}}^{\Delta_{n,ij}^{(\mathrm{up})}} f(u)du, \tag{34}$$

the errors for k^{th} moments $E_{\Delta t}^{(k)}$ can be written as

$$\begin{aligned}\left|\mathrm{R}_{\Delta t,m}^{(k)}\right| &= \left|\sum_{j=1}^m p_{ij}^n\left(X_j^{n+1} - X_i^n\right)^k - \int_{-\infty}^{+\infty} u^k\rho^{GH_{\Delta t}}(u)du\right| \\ &\leq \sum_{j=1}^m\left|\mathcal{I}\left[\left(\left(\Delta X_{ij}^n\right)^k - u^k\right)\rho^{GH_{\Delta t}}(u)\right]\right| = \sum_{\ell=1}^{k-1}\frac{k!}{\ell!(k-\ell)!}\sum_{j=1}^m\left|\mathcal{I}\left[u^\ell\left(\Delta X_{ij}^n - u\right)^{k-\ell}\rho^{GH_{\Delta t}}(u)\right]\right|.\end{aligned} \tag{35}$$

Thanks to Cauchy–Schwarz inequality and Lemma 6, we have

$$
\begin{aligned}
\left|R_{\Delta t,m}^{(k)}\right| &\le \sum_{\ell=1}^{k-1} \frac{k!}{\ell!(k-\ell)!} \sum_{j=1}^{m} \left| \mathcal{I}\left[u^{\ell} \left(\Delta X_{ij}^{n} - u\right)^{k-\ell} \rho^{GH_{\Delta t}}(u) \right] \right| \\
&\le \sum_{\ell=1}^{k-1} \frac{k!}{\ell!(k-\ell)!} \left\{ \sum_{j=1}^{m} \mathcal{I}\left(u^{2\ell} \rho^{GH_{\Delta t}}(u) \right) \right\}^{1/2} \left\{ \sum_{j=1}^{m} \mathcal{I}\left[\left(\Delta X_{ij}^{n} - u\right)^{2(k-\ell)} \rho^{GH_{\Delta t}}(u) \right] \right\}^{1/2} \\
&\le \sum_{\ell=1}^{k-1} \frac{k!}{\ell!(k-\ell)!} \left[E_{\Delta X}^{(2\ell)} \right]^{1/2} \left\{ \sum_{j=1}^{m} h_{j}^{2(k-\ell)} \mathcal{I}\left[\rho^{GH_{\Delta t}}(u) \right] \right\}^{1/2} \\
&\le \sum_{\ell=1}^{k-1} \frac{k!}{\ell!(k-\ell)!} \left[E_{\Delta X}^{(2\ell)} \right]^{1/2} \left(\frac{H}{m} \right)^{k-\ell} = O\left(\frac{\sqrt{\Delta t}}{m} \right), \quad k \ge 1,
\end{aligned}
\tag{36}
$$

which is the result of (33). □

The following theorem gives the error estimation of the willow tree algorithm for European options.

Theorem 9. *Given the asset price S_t governed by the exponential Lévy model $S_t = S_0 e^{(r+\omega_{GH})t + X_t}$, on discrete times $0 = t_0 < t_1 < t_2 < \cdots < t_N = T$ with $\Delta t = T/N$ and m discrete values X_i^n being generated by (9). If h satisfies conditions in Assumption 5, the error between the true value $V(x,t)$ of the European option and the computed value $\overline{V}(x,t)$ by the backward induction (19) in the willow tree is $O(\Delta t) = O(1/N)$ when m is in $O(\Delta t^{-3/2}) = O(N^{3/2})$.*

Proof. It is known that the European option $V(y,t)$ with $y = \log S(t)$ is the solution of the following partial integrodifferential equation (PIDE):

$$
V_t(y,t) + (r + \omega_{\mathrm{GH}}) V_y(y,t) - rV(y,t) + \int_{-\infty}^{\infty} [V(y+\theta,t) - V(y,t)] \Pi(d\theta) = 0, \tag{37}
$$

with the terminal condition $V(y,T) = f(y)$, ($f(y) = (e^y - K)^+$ for call option or $f(y) = (K - e^y)^+$ for put option), and $\Pi(d\theta)$ being the Lévy measure (see Lévy representation Theorem 2.7 in [7]). Given willow tree, the European option $\overline{V}(y_i^n, t_n)$ with $y_i^n = \log S_i^n = (r + \omega_{\mathrm{GH}}) t_n + X_i^n$ is computed by the backward induction as in (19), i.e.,

$$
\overline{V}(y_i^n, t_n) = e^{-r\Delta t} \sum_{j=1}^{m} p_{ij}^{(n)} \overline{V}\left(y_j^{n+1}, t_{n+1}\right). \tag{38}
$$

Expanding $\overline{V}(y_j^{n+1}, t_{n+1})$ at (y_i^n, t_n) by the Taylor series, we have

$$
\begin{aligned}
\overline{V}\left(y_j^{n+1}, t_{n+1}\right) &= \overline{V}(y_i^n, t_n) + \overline{V}_t(y_i^n, t_n)\Delta t + \overline{V}_y(y_i^n, t_n)\Delta Y_{ij}^n + \frac{1}{2}\overline{V}_{yy}(y_i^n, t_n)\left(\Delta Y_{ij}^n\right)^2 \\
&\quad + \frac{1}{6} \frac{\partial^3 \overline{V}(\xi, t_n)}{\partial y^3} \left(\Delta Y_{ij}^n\right)^3 + O\left((\Delta t)^2\right) + O\left(\Delta Y_{ij}^n \Delta t\right),
\end{aligned}
\tag{39}
$$

where $\Delta Y_{ij}^n = y_j^{n+1} - y_i^n$ and $\xi \in (y_i^n, y_i^n + \Delta Y_{ij}^n)$. Thus, the backward induction (38) can be written as

$$\begin{aligned}\overline{V}\left(y_i^n,t_n\right) &= e^{-r\Delta t}\sum_{j=1}^{m} p_{ij}^{(n)}\overline{V}\left(y_j^{n+1},t_{n+1}\right)\\ &= (1-r\Delta t)\sum_{j=1}^{m} p_{ij}^{(n)}\left[\overline{V}\left(y_i^n,t_n\right)+\overline{V}_t\left(y_i^n,t_n\right)\Delta t+\overline{V}_y\left(y_i^n,t_n\right)\Delta Y_{ij}^n\right]\\ &\quad+(1-r\Delta t)\sum_{j=1}^{m} p_{ij}^{(n)}\left[\frac{1}{2}\overline{V}_{yy}\left(y_i^n,t_n\right)\left(\Delta Y_{ij}^n\right)^2+\frac{1}{6}\frac{\partial^3\overline{V}\left(\xi,t_n\right)}{\partial y^3}\left(\Delta Y_{ij}^n\right)^3\right]\\ &\quad+O\left((\Delta t)^2\right)+O\left(\sum_{j=1}^{m} p_{ij}^{(n)}\Delta Y_{ij}^n\Delta t\right).\end{aligned}\tag{40}$$

From Lemma 8, the discrete approximation of the first- and second-order moments of the GH process can be estimated as

$$\begin{aligned}\sum_{j=1}^{m} p_{ij}^{(n)}\Delta Y_{ij}^n &= E_{\Delta t}^{(1)}+O\left(\frac{\sqrt{\Delta t}}{m}\right)\\ &= \left(r+\omega_{\mathrm{GH}}\right)\Delta t+\Delta t\mathbb{E}\left[X_t\right]\\ &\quad+O\left(\frac{\sqrt{\Delta t}}{m}\right),\end{aligned}\tag{41}$$

$$\begin{aligned}\sum_{j=1}^{m} p_{ij}^{(n)}\left(\Delta Y_{ij}^n\right)^2 &= E_{\Delta t}^{(2)}+O\left(\frac{\sqrt{\Delta t}}{m}\right)\\ &= \Delta t\mathrm{Var}\left[X_t\right]+O\left(\frac{\sqrt{\Delta t}}{m}\right),\end{aligned}\tag{42}$$

$$\sum_{j=1}^{m} p_{ij}^{(n)}\left(\Delta Y_{ij}^n\right)^k = E_{\Delta t}^{(k)}+O\left(\frac{\sqrt{\Delta t}}{m}\right),\quad k\geq 3.\tag{43}$$

From (40)–(43), we have

$$\begin{aligned}&\overline{V}_t\left(y_i^n,t_n\right)+\left[\left(r+\omega_{GH}\right)+\frac{1}{\Delta t}E_{\Delta t}^{(1)}\right]\overline{V}_y\left(y_i^n,t_n\right)-r\overline{V}\left(y_i^n,t_n\right)+\frac{1}{2\Delta t}E_{\Delta t}^{(2)}\overline{V}_{yy}\left(y_i^n,t_n\right)\\ &\quad+\frac{1}{6\Delta t}E_{\Delta t}^{(3)}\frac{\partial^3\overline{V}\left(\xi,t_n\right)}{\partial y^3}+O(\Delta t)+O\left(\frac{\sqrt{\Delta t}}{m}\right)=0\text{with}\xi\in\left(y_i^n,y_i^n+\Delta Y_{ij}^n\right).\end{aligned}\tag{44}$$

On the other hand, using the Taylor expansion of $\overline{V}\left(y_i^n+\theta,t_n\right)$ at $\left(y_i^n,t_n\right)$, we have

$$\overline{V}\left(y_i^n+\theta,t_n\right)-\overline{V}\left(y_i^n,t_n\right)=\overline{V}_y\left(y_i^n,t_n\right)\theta+\frac{1}{2}\overline{V}_{yy}\left(y_i^n,t_n\right)\theta^2+\frac{1}{6}\frac{\partial^3\overline{V}\left(\xi,t_n\right)}{\partial y^3}\theta^3,\tag{45}$$

with $\xi\in\left(y_i^n,y_i^n+\Delta Y_{ij}^n\right)$. Applying the properties of Lévy measure, it is obtained that

$$\int_{-\infty}^{\infty}\theta^k\Pi(d\theta)=\frac{1}{\Delta t}E_{\Delta t}^{(k)}+O\left((\Delta t)^k\right),\quad k\geq 1.\tag{46}$$

Table 3: Parameters of the GH model for some special cases.

Model	λ	α	β	δ	μ
GH	−2	15	8	0.3	0.7
HYP	1	15	8	0.3	0.7
NIG	−0.5	15	8	0.3	0.7
VG	−1.5	15	12	0.0001	0.0001

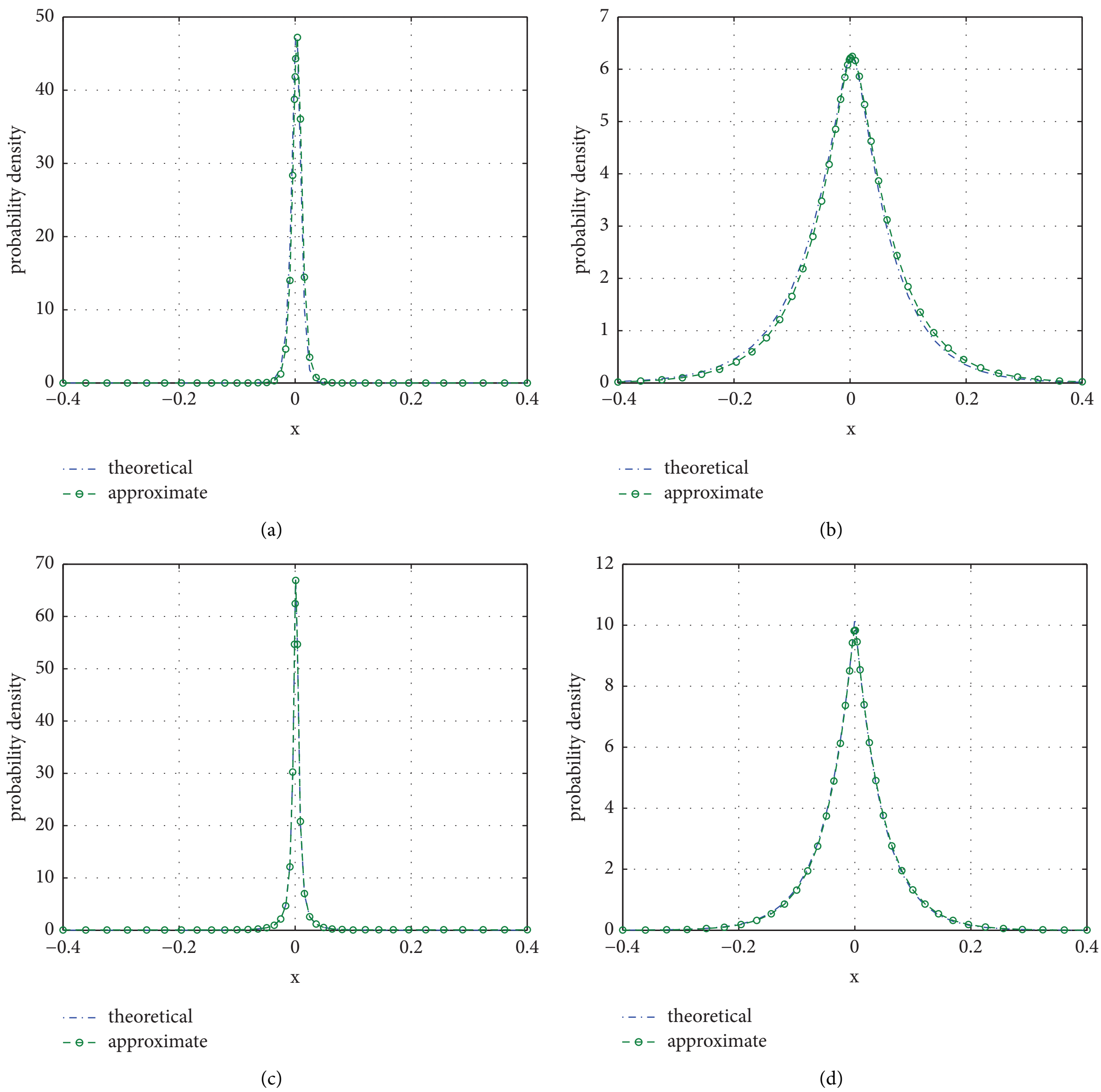

Figure 3: Density functions under (a) GH, (b) HYP, (c) NIG, and (d) VG models. All parameters of these models are listed in Table 3.

Therefore, using (45) and (46), it is yielded that

$$\begin{aligned}&\int_{-\infty}^{\infty}[\overline{V}(y_i^n+\theta,t_n)-\overline{V}(y_i^n,t_n)]\Pi(d\theta)\\&=\frac{1}{\Delta t}E_{\Delta t}^{(1)}\overline{V}_y(y_i^n,t_n)+\frac{1}{2\Delta t}E_{\Delta t}^{(2)}\overline{V}_{yy}(y_i^n,t_n)+\frac{1}{6\Delta t}E_{\Delta t}^{(3)}\frac{\partial^3\overline{V}(\xi,t_n)}{\partial y^3}+O(\Delta t).\end{aligned}\tag{47}$$

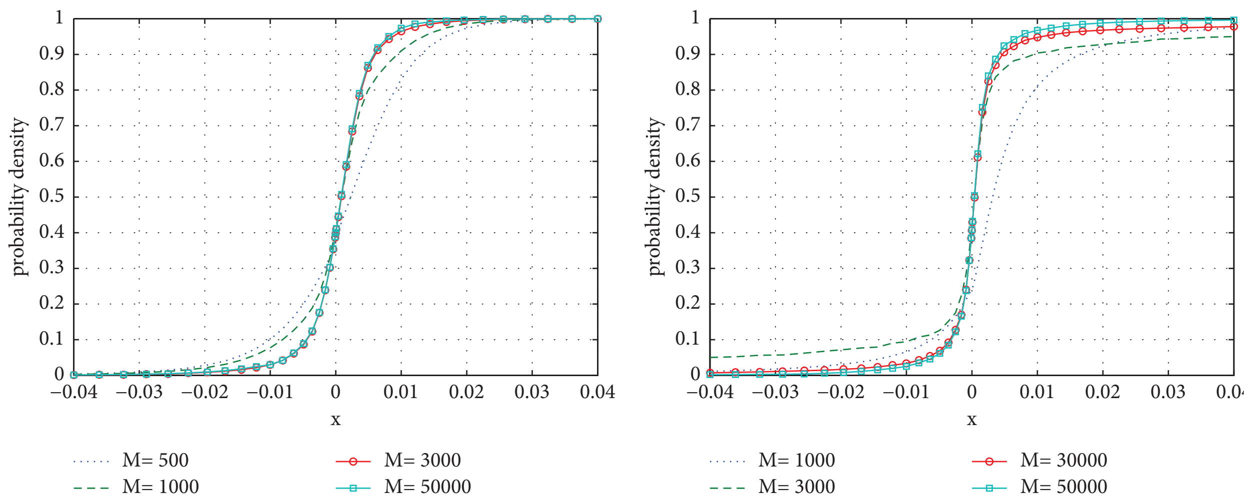

(a) (b)

FIGURE 4: Cumulative distribution functions of (a) GH model and (b) NIG model with $\Delta t = 0.25$ and different number of M. All parameters of two models are listed in Table 3.

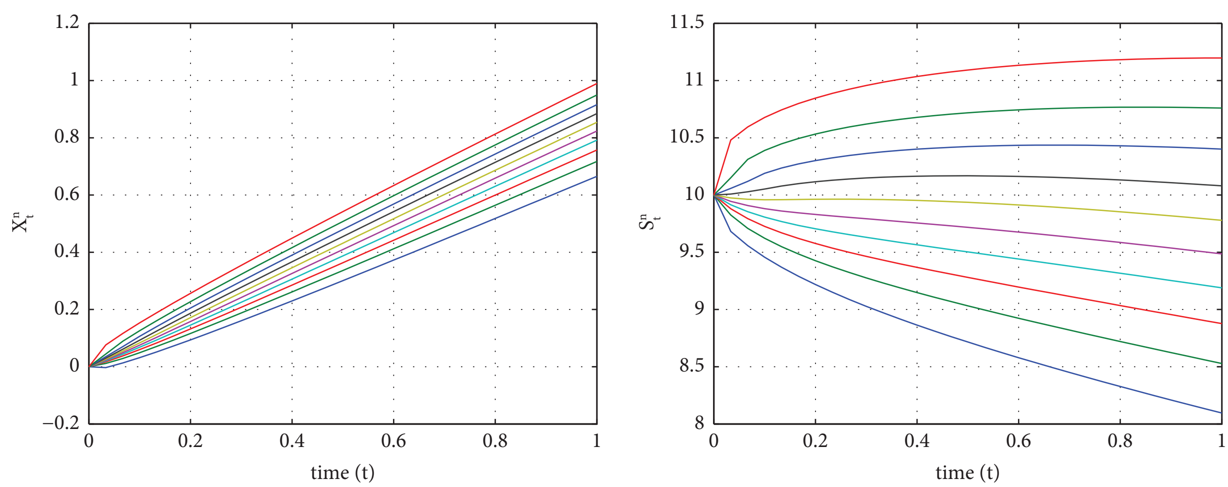

(a) (b)

FIGURE 5: Trajectories of X_t and S_t for the NIG model with $m = 10$ and $N = 30$: (a) nodes X_t^n and (b) nodes S_t^n.

Combining (44) and (47), we have

$$\begin{aligned} &\overline{V}_t\left(y_i^n, t_n\right) + \left(r + \omega_{GH}\right)\overline{V}_y\left(y_i^n, t_n\right) - r\overline{V}\left(y_i^n, t_n\right) \\ &+ \int_{-\infty}^{\infty} \left[\overline{V}\left(y_i^n + \theta, t_n\right) - \overline{V}\left(y_i^n, t_n\right)\right]\Pi\left(d\theta\right) + O\left(\Delta t\right) + O\left(\frac{1}{m\sqrt{\Delta t}}\right) = 0, \end{aligned} \tag{48}$$

at all nodes (y_i^n, t_n). Comparing (48) with (37), we see any European option value $\overline{V}(y_i^n, t_n)$ computed by the backward induction (38) satisfies PIDE (37) with error term $O(\Delta t) + O(1/m\sqrt{\Delta t})$. When m is in $O(\Delta t^{-3/2})$, the error term $O(\Delta t) + O(1/m\sqrt{\Delta t})$ is emerged as $O(\Delta t) = O(1/N)$. □

Remark 10. To obtain option values with good accuracy, the number of m should be taken as $\mathcal{O}(N^{3/2})$. Since European options are path-independent, the number of N should be selected as small as possible, whereas the number m should be taken as large enough since N should be taken as large as possible for American options.

Table 4: Option values calculated by WT method, MC method, and analytical formulas.

K	ECWT	ECMC	ECA	ERR	K	APWT	APMC	ERR
GH model								
2.00	2.6349	2.6352	—	$2.50e-04$	10.00	0.4280	0.4365	$8.53e-03$
2.50	2.1497	2.1499	—	$2.50e-04$	10.50	0.7160	0.7260	$9.96e-03$
3.00	1.6645	1.6647	—	$2.50e-04$	11.00	1.0796	1.0888	$9.19e-03$
3.50	1.1793	1.1795	—	$2.50e-04$	11.50	1.5101	1.5159	$5.76e-03$
CPU(s)	3.14	32.53	—	—	—	3.14	311.05	—
HYP model								
2.00	1.9754	1.9754	—	$4.06e-06$	10.00	0.7461	0.7486	$2.47e-03$
2.50	1.4901	1.4901	—	$4.06e-06$	10.50	1.0401	1.0424	$2.31e-03$
3.00	1.0049	1.0049	—	$4.06e-06$	11.00	1.3759	1.3788	$2.89e-03$
3.50	0.5198	0.5198	—	$9.49e-06$	11.50	1.7479	1.7511	$3.16e-03$
CPU(s)	2.78	23.02	—	—	—	2.90	290.50	—
NIG model								
2.00	2.3485	2.3488	2.3487	$3.27e-04$	10.00	0.5662	0.5672	$9.96e-04$
2.50	1.8632	1.8636	1.8636	$3.27e-04$	10.50	0.8566	0.8584	$1.87e-03$
3.00	1.3780	1.3783	1.3784	$3.27e-04$	11.00	1.2025	1.2059	$3.40e-03$
3.50	0.8928	0.8931	0.8932	$3.27e-04$	11.50	1.5961	1.6000	$3.91e-03$
CPU(s)	0.82	18.48	—	—	—	9.77	169.23	—
VG model								
2.00	8.0583	8.0587	8.0588	$4.30e-04$	10.00	0.1033	0.1016	$1.73e-03$
2.50	7.5731	7.5735	7.5375	$4.30e-04$	10.50	0.5000	0.5000	0.00e+00
3.00	7.0879	7.0883	7.0884	$4.30e-04$	11.00	1.0000	1.0000	$0.00e+00$
3.50	6.6026	6.6031	6.6032	$4.30e-04$	11.50	1.5000	1.5000	$0.00e+00$
CPU(s)	0.82	18.48	—	—	—	9.59	169.23	—

European call options by WT, MC methods, and analytical formula are labeled by "ECWT," "ECMC," and "ECA," respectively. American put options by WT and MC methods are labeled by "APWT" and "APMC," respectively. ERRs are the corresponding errors between the WT method and Monte Carlo method.

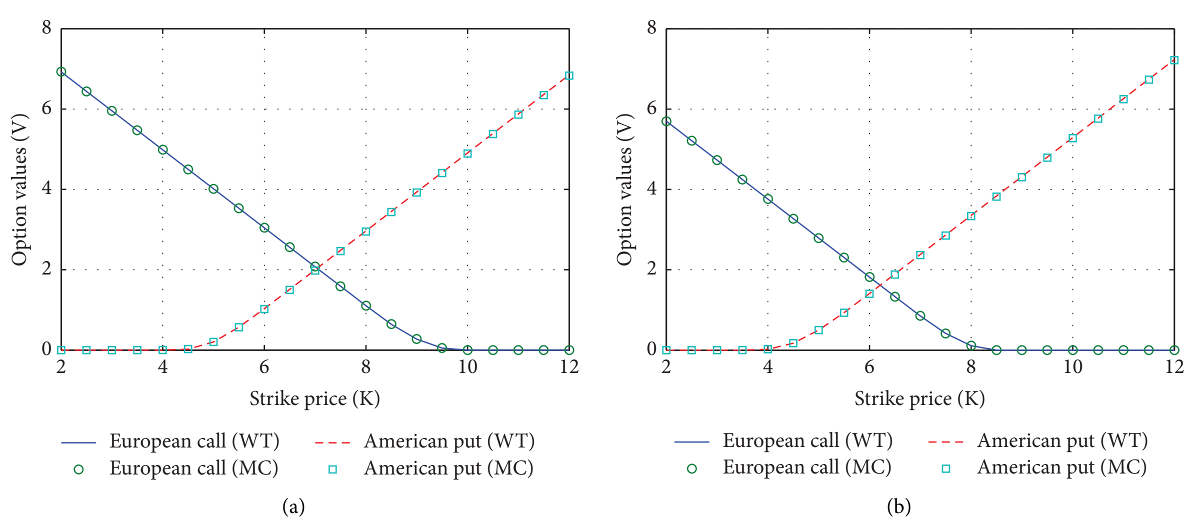

Figure 6: Continued.

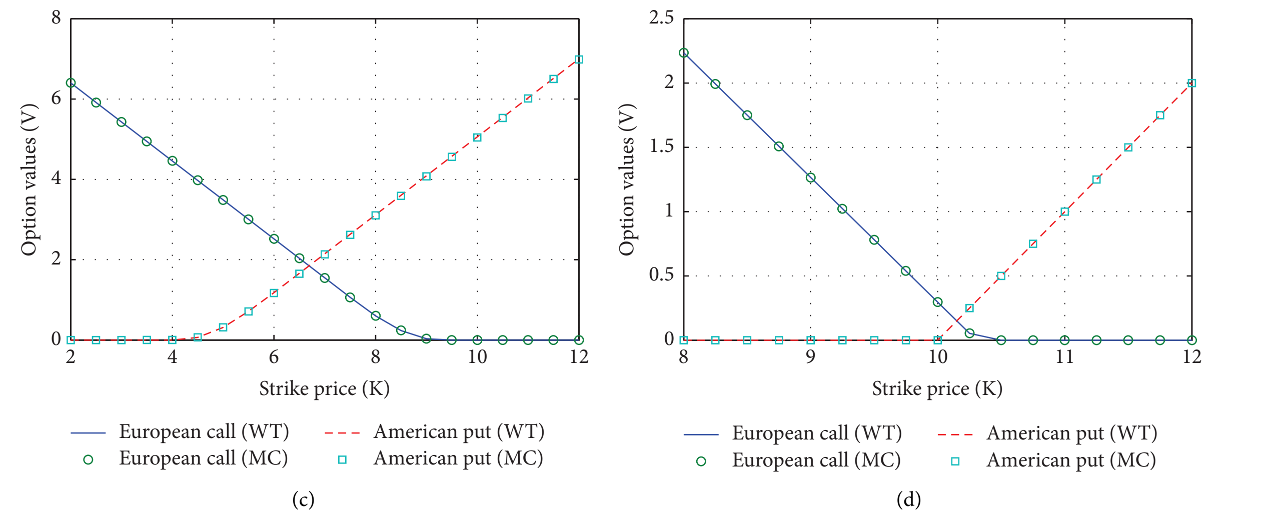

FIGURE 6: European call and American put option values under. (a) GH model, (b) HYP model, (c) NIG model, and (d) VG model. All parameters of these models are listed in Table 3.

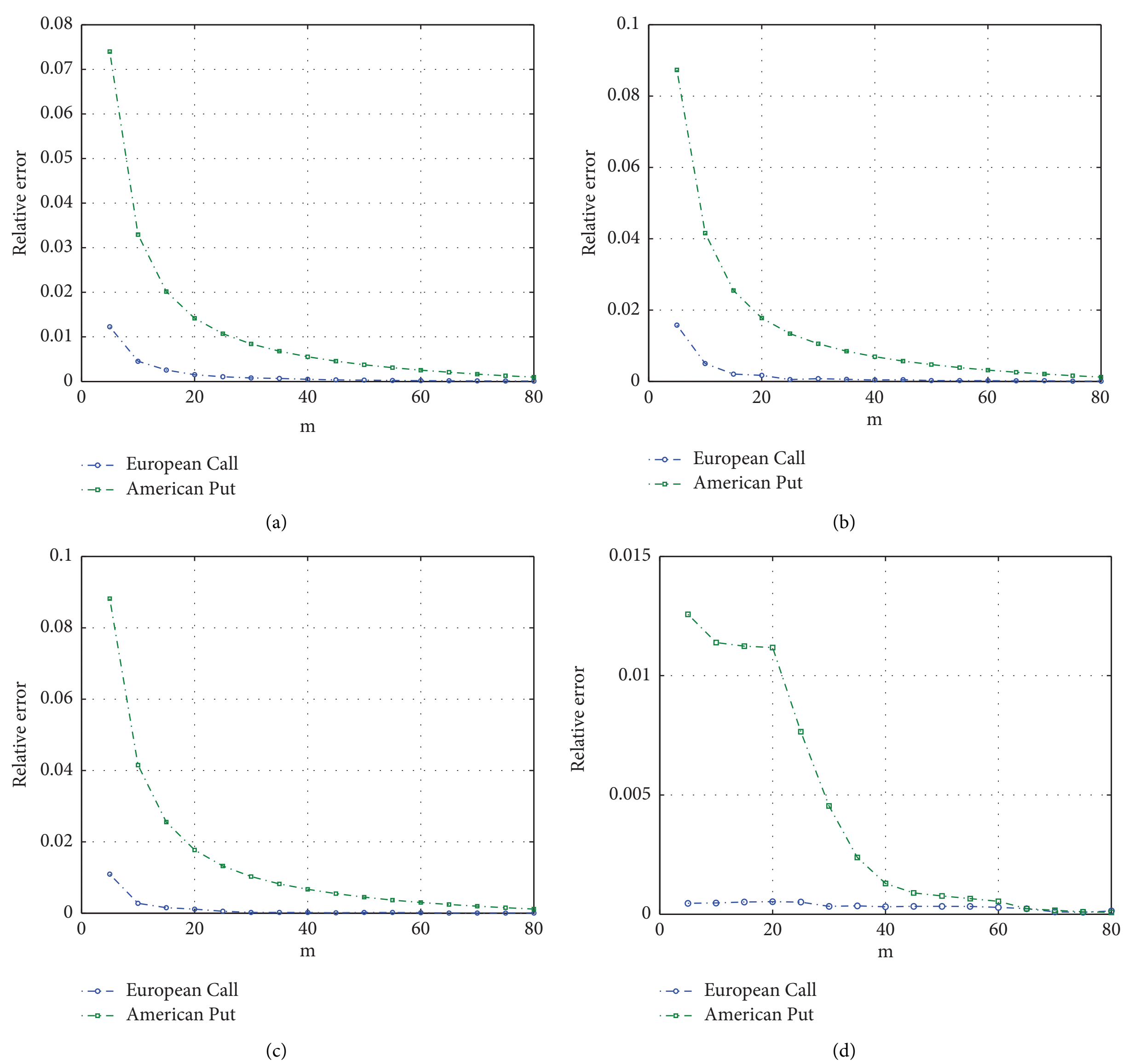

FIGURE 7: Convergence of willow tree with respect to *m*. All parameters are listed in Table 3: (a) GH model, (b) HYP model, (c) NIG model, and (d) VG model.

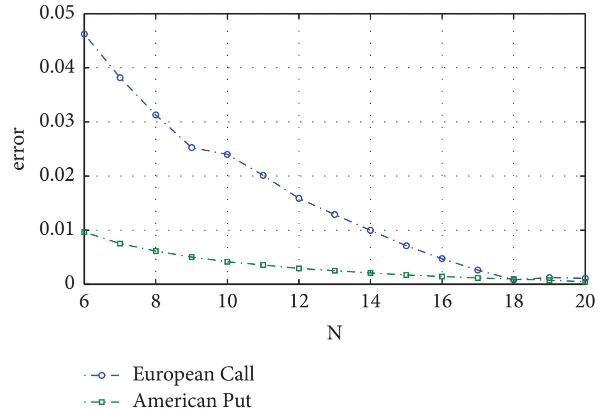

(a)

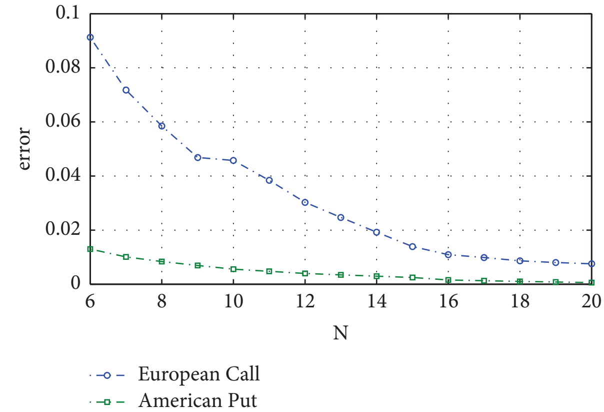

(b)

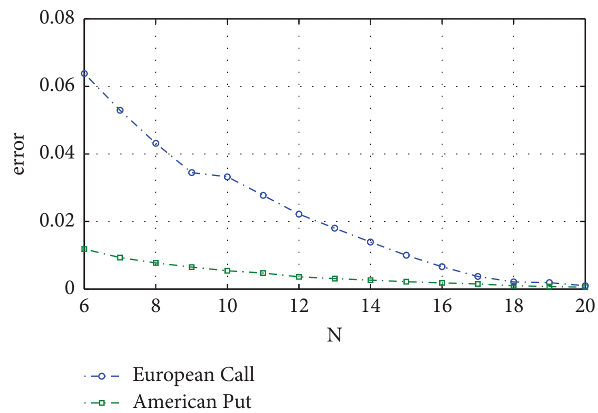

(c)

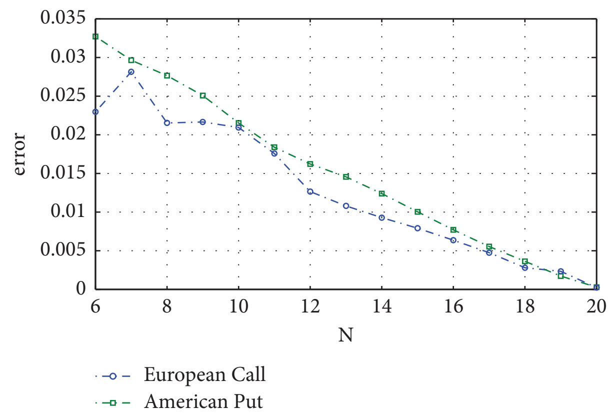

(d)

Figure 8: Convergence of willow tree with respect to N with fixed $m = 50$. All parameters are listed in Table 3: (a) GH model, (b) HYP model, (c) NIG model, and (d) VG model.

5. Numerical Examples

To test the performance of the willow tree (WT) method for option valuating, we consider four classes of choices (GH, HYP, NIG, and VG models) with parameters being listed in Table 3. Parameters of risk-free interest, initial stock price, and maturity time are set as $r = 0.03, S_0 = 10, T = 1$. ($N = 1, m = 200$) are set in the WT algorithm for European options, whereas ($N = 100, m = 200$) for American options. In Monte Carlo (MC) simulation, ($N_{\mathrm{mc}} = 100, M_{\mathrm{mc}} = 5,000,000$) are set with N_{mc} representing the number of time partition and M_{mc} represents the number of simulated paths. In numerical formula (14), we set numerical partition $M = 50,000$ for variable u of characteristic functions.

All experiments are carried out by MATLAB R2012b running on a machine with Intel(R) Core (TM) i7-8550U CPU @ 1.80 GHz, 8 GB RAM under Windows 10.

Figure 3 plots probability density functions (PDFs) of GH, HYP, NIG, and VG models with $t = 1$. The figure shows that the PDFs computed from numerical formula (14) are very close to explicit expression (3). So, we believe that PDFs $\rho^{\mathrm{GH}_t}(x)$ computed from (14) with time $t = \Delta t$ are also accurate enough. Figure 4 plots the shape of cumulative distribution functions (CDFs) with different numbers of M, from which we see the computed CDFs are convergent as M becoming larger. Figure 5 plots the trajectories of nodes X_t^n and S_t^n for the NIG model.

Option values computed from WT algorithms, MC simulations, and analytical solutions (labeled by "ECA") are listed in Table 4. Figure 6 plots values of European and American options, from which we see WT solutions are very close to those obtained by MC simulation. We see that the errors between WT solution and analytical solutions (or MC solutions) are about 10^{-3}. In European options computation, the CPU time consumed from WT is less than 3 seconds whereas more than 18 s for MC simulation. In American option computation, the CPU time consumed from WT is less than 10 s, whereas more than 160 s for the MC method. The results in Table 4 illustrate the effectiveness of the proposed WT method. The analytical formula of European options under NIG and VG processes can be seen in literatures [2, 6, 28, 29]. Those pricing formulas are also listed in Appendix A and Appendix B.

To test the convergence of the willow tree method with respect to the number m of space nodes and time partition number N, some experiments are carried out. Figure 7 plots the errors for different parameters m with fixed $N = 20$.

Table 5: Convergence rate for time partition N.

N	m	Err (Eu)	Conv. rate	Err (Am)	Conv. rate
GH model					
5	55	0.1147	1.192	0.0302	1.019
10	158	0.0502	1.072	0.0149	1.033
15	290	0.0325	1.151	0.0098	0.976
20	447	0.0233	—	0.0074	—
HYP model					
5	55	0.0823	1.009	0.0252	1.095
10	158	0.0409	1.089	0.0118	1.021
15	290	0.0263	1.058	0.0078	1.012
20	447	0.0194	—	0.0058	—
NIG model					
5	55	0.0732	1.016	0.0145	0.998
10	158	0.0362	1.097	0.0073	1.062
15	290	0.0232	1.206	0.0047	1.069
20	447	0.0164	—	0.0035	—
VG model					
5	55	0.1256	1.012	0.1423	0.985
10	158	0.0623	0.996	0.0719	1.054
15	290	0.0416	1.045	0.0469	1.037
20	447	0.0308	—	0.0348	—

The corresponding underlying discretization $m = [N^{3/2}]$. All parameters of these models are listed in Table 3.

Figure 8 plots the errors with different N and corresponding $m = [N^{3/2}]$, from which we see the errors are decreasing as N (and so m) increases. Table 5 lists the numerical convergent rates with respect to the values of N. These results in Figures 7 and 8 and Table 5 support the theoretical conclusion in Theorem 9.

6. Conclusions

In this paper, a unified and robust approach is proposed to construct the willow tree structure for GH Lévy processes. There are two advantages of our proposed approach compared to that in [19]. First, it avoids the moment matching failure by the Johnson curve under some circumstances in the willow tree construction. Second, the error of European call option pricing is only determined by Δt. The fifth-moment term of Lévy measure is removed from the error bound, so our approach improves the stability and accuracy of the willow tree in option pricing. Numerical experiments support our claims.

Moreover, we believe the proposed willow tree method can be extended to other option models, such as variance and volatility swaps with stochastic volatility and stochastic volatility model with regime switching stochastic mean reversion (see, e.g., [30–33]). We will discuss those models in the future.

Appendix

A. Analytical Solution under VG Model

When the risk-neutral dynamics of the stock price is given by the VG process (for risk-neutral parameters σ, ν, θ), the European call option price on a stock is (see page 88 in [2]):

$$C(S;K,t) = S\Psi\left(d\sqrt{\frac{1-C_1}{\nu}}, (\alpha+s)\sqrt{\frac{\nu}{1-C_1}}, \frac{t}{\nu}\right) - Ke^{-rt}\Psi\left(d\sqrt{\frac{1-C_2}{\nu}}, \alpha S\sqrt{\frac{\nu}{1-C_2}}, \frac{t}{\nu}\right), \quad (A.1)$$

where $\alpha = \zeta s$,

$$\begin{aligned} \zeta &= -\frac{\theta}{\sigma^2}, \\ s &= \frac{\sigma}{\sqrt{1+\nu(\theta/2)^2/2}}, \\ C_1 &= \frac{\nu(\alpha+s)^2}{2}, \\ C_2 &= \frac{\nu\alpha^2}{2}, \end{aligned} \quad (A.2)$$

and $\Psi(\cdot,\cdot,\cdot)$ is defined in terms of the modified Bessel function of the second kind.

B. Analytical Solution under NIG Model

When the risk-neutral dynamics of the stock price is given by NIG, the European call option price is (see Theorem 2.1, Theorem 2.2, and Corollary 2.1 in Ivanov [6])

$$C = \mathrm{DAC} - \mathrm{DCC}, \quad (B.1)$$

with definitions

$$\begin{aligned} \mathrm{DAC} &= \frac{A\sqrt{D}}{\pi\sqrt{2}}\beta\left(\frac{1}{2},1\right)K_1(A)e^A\Phi\left(\frac{1}{2},\frac{1}{2},\frac{3}{2};\frac{D}{2},-A-\frac{rT-\log K}{2}\right) \\ &\quad + \frac{\mathrm{AD}\sqrt{D}}{\pi\sqrt{2}}\beta\left(\frac{3}{2},1\right)K_0(A)e^A\Phi\left(\frac{3}{2},\frac{1}{2},\frac{5}{2};\frac{D}{2},-A-\frac{rT-\log K}{2}\right) \\ &\quad - \frac{A\sqrt{D}}{\pi\sqrt{2}}\beta\left(\frac{1}{2},1\right)K_0(A)e^A\Phi\left(\frac{1}{2},\frac{1}{2},\frac{3}{2};\frac{D}{2},-A-\frac{rT-\log K}{2}\right), \\ A &= \frac{1}{2}\left[(rT-\log K)^2+(\delta T)^2\right]^{1/2}, \quad D = \frac{1}{2A}\left[rT-\log K+2A\right], \end{aligned} \tag{B.2}$$

and

$$\mathrm{DCC} = \mathrm{DAC}\cdot Ke^{-rT-2A}. \tag{B.3}$$

In the above formula, $K_\gamma(x)$ is the MacDonald function, $\beta(x,y)$ is the beta function, and $\Phi(\gamma_1,\gamma_2,\gamma_3;x,y)$ is the degenerate Appell hypergeometric function.

Data Availability

The authors confirm that the data supporting the findings of this study are available within the article.

Conflicts of Interest

The authors declare that there are no conflicts of interest regarding the publication of this paper.

Acknowledgments

This work was supported by the National Natural Science Foundation of China (grant no. 12171409) and Key Project of Hunan Education Department (grant no. 238945).

References

[1] E. Eberlein, U. Keller, and K. Prause, "New insights into smile, mispricing and value at risk: the hyperbolic model," *Journal of Business*, vol. 71, no. 3, pp. 371–405, 1998.

[2] D. Madan, P. Carr, and E. Chang, "The variance Gamma process and option pricing," *Review of Finance*, vol. 2, no. 1, pp. 79–105, 1998.

[3] S. Muzziol and B. De Baets, "The variance-gamma process for option pricing," *European Journal of Operational Research*, vol. 2, pp. 63–71, 1999.

[4] O. Barndorff-Nielsen, "Normal inverse Gaussian distributions and stoch-astic volatility modelling," *Scandinavian Journal of Statistics*, vol. 24, no. 1, pp. 1–13, 1997.

[5] O. Barndorff-Nielsen, "Processes of normal inverse Gaussian type," *Finance and Stochastics*, vol. 2, no. 1, pp. 41–68, 1997.

[6] R. V. Ivanov, "Closed form pricing of European options for a family of normal- inverse Gaussian processes," *Stochastic Models*, vol. 29, no. 4, pp. 435–450, 2013.

[7] A. Kumar, M. M. Meerschaert, and P. Vellaisamy, "Fractional normal inverse Gaussian diffusion," *Statistics & Probability Letters*, vol. 81, no. 1, pp. 146–152, 2011.

[8] L. Jiang and M. Dai, "Convergence of Binomial tree methods for European/American path-dependent options," *SIAM Journal on Numerical Analysis*, vol. 42, no. 3, pp. 1094–1109, 2004.

[9] S. Muzzioli and C. Torricelli, "The pricing of options on an interval binomial tree: an application to the dax-index option market," *European Journal of Operational Research*, vol. 163, no. 1, pp. 192–200, 2005.

[10] J. Ma and Z. Zhou, "Fast Laplace transform methods for the PDE system of Parisian and Parasian option pricing," *Science China Mathematics*, vol. 65, no. 6, pp. 1229–1246, 2022.

[11] Z. Zhou, J. Ma, and X. Gao, "Convergence of iterative laplace transform methods for a system of fractional PDEs and PIDEs arising in option pricing," *East Asian Journal on Applied Mathematics*, vol. 8, no. 4, pp. 782–808, 2018.

[12] Z. Zhou, J. Ma, and H. Sun, "Fast Laplace transform methods for free-boundary problems of fractional diffusion equations," *Journal of Scientific Computing*, vol. 74, no. 1, pp. 49–69, 2018.

[13] Z. Zhou, W. Xu, and A. bRubtsov, "Joint calibration of S&P 500 and VIX options under local stochastic volatility models," *International Journal of Finance & Economics*, vol. 1–38, 2022.

[14] L. Ballotta and I. Kyriakou, "Monte Carlo simulation of the CGMY process and option pricing," *Journal of Futures Markets*, vol. 34, no. 12, pp. 1095–1121, 2014.

[15] M. C. Chiu, W. Y. Wang, and H. Y. Wong, "FFT-network for bivariate Lévy option pricing," *Japan Journal of Industrial and Applied Mathematics*, vol. 38, no. 1, pp. 323–352, 2020.

[16] H. Jonsson, C. Oosterlee, and W. Schoutens, "Fast valuation and calibration of credit default swaps under Lévy dynamics," *Journal of Computational Finance*, vol. 14, no. 2, pp. 57–86, 2010.

[17] J. Kirkby, "American and exotic option pricing with jump diffusions and other Lévy processes," *Journal of Computational Finance*, vol. 22, no. 3, pp. 89–148, 2018.

[18] H. Y. Wong and P. Guan, "An FFT-network for Lévy option pricing," *Journal of Banking & Finance*, vol. 35, no. 4, pp. 988–999, 2011.

[19] J. Ma, W. Xu, and Y. Yao, "Cosine willow tree structure under Lévy processes with application to pricing variance derivatives," *Journal of Derivatives*, vol. 29, no. 2, pp. 30–60, 2021.

[20] A. Hirsa, *Computational Methods in Finance*, CRC Press, Boca Raton, FL, USA, 2016.

[21] Z. Zhou and W. Xu, "Robust willow tree method under Lévy processes," *Journal of Computational and Applied Mathematics*, vol. 424, no. 3–19, Article ID 114982, 2023.

[22] J. Imai and K. Tan, "An accelerating Quasi-Monte Carlo method for option pricing under the generalized hyperbolic Lévy process," *SIAM Journal on Scientific Computing*, vol. 31, no. 3, pp. 2282–2302, 2009.

[23] Y. Kwok and W. Zheng, *Pricing Models of Volatility Products and Exotic Variance Derivatives*, Springer, Berlin, Germany, 2020.
[24] K. Sato, *Lévy Processes and Infinitely Divisible Distributions*, Cambridge University Press, Cambridge, UK, 1999.
[25] W. Schoutens, *Lévy Processes in Finance: Pricing Financial Derivatives*, John Wiley and Sons, New York, NY, USA, 2003.
[26] L. Richard and J. Dougals Faires, *Numerical Analysis*, Thomson Learning, Inc, Chicago, IL, USA, 2001.
[27] R. Cont and P. Tankov, *Financial Modelling with Jump Processes*, CRC press LLC, Boca Raton, FL, USA, 2016.
[28] A. Bilgi Yilmaz and A. Alper Hekimoglu, "Sevtap Selcuk-Kestel, Default and prepayment options pricing and default probability valuation under VG model," *Journal of Computational and Applied Mathematics*, vol. 399, 2022.
[29] Y. S. Kim, "Tempered stable process, first passage time, and path-dependent option pricing," *Computational Management Science*, vol. 16, no. 1-2, pp. 187–215, 2019.
[30] X. J. He and S. Lin, "Analytically pricing exchange options with stochastic liquidity and regime switching," *Journal of Futures Markets*, vol. 43, no. 5, pp. 662–676, 2023.
[31] X. J. He and S. Lin, "A new nonlinear stochastic volatility model with regime switching stochastic mean reversion and its applications to option pricing," *Expert Systems with Applications*, vol. 212, Article ID 118742, 2023.
[32] X. J. He and S. Lin, "A closed-form pricing formula for European options under a new three-factor stochastic volatility model with regime switching," *Japan Journal of Industrial and Applied Mathematics*, vol. 40, no. 1, pp. 525–536, 2023.
[33] S. Lin and X. J. He, "Analytically pricing variance and volatility swaps with stochastic volatility, stochastic equilibrium level and regime switching," *Expert Systems with Applications*, vol. 217, Article ID 119592, 2023.